

**Processing of amorphous carbon films by ultrafast temperature treatment in a confined geometry**

J. A. Lenz, C. A. Perotoni, N. M. Balzaretti, and J. A. H. da Jornada

Citation: [Journal of Applied Physics](#) **89**, 8284 (2001); doi: 10.1063/1.1374457

View online: <http://dx.doi.org/10.1063/1.1374457>

View Table of Contents: <http://scitation.aip.org/content/aip/journal/jap/89/12?ver=pdfcov>

Published by the [AIP Publishing](#)

---



## Re-register for Table of Content Alerts

Create a profile.



Sign up today!



# Processing of amorphous carbon films by ultrafast temperature treatment in a confined geometry

J. A. Lenz

CEFET-PR-Uned Medianeira-Medianeira PR-85884-000-Brazil

C. A. Perottoni,<sup>a)</sup> N. M. Balzaretto,<sup>b)</sup> and J. A. H. da Jornada<sup>a)</sup>

Instituto de Física, UFRGS—Porto Alegre, RS, CP 15051-91501 970-Brazil

(Received 31 October 2000; accepted for publication 2 April 2001)

A pressure cell with an anvil made of sapphire and the other made of tungsten carbide, was constructed to process thin film samples using a high power Nd:YAG pulsed laser, in a regime of ultrafast quenching rate and confined geometry. The sapphire anvil worked as the optical window to the laser beam and also as a good thermal conductor substrate. Thin films of amorphous carbon deposited over copper substrate were processed under pressure by Nd:YAG laser pulses. This process induces the formation of a high temperature region at the sample surface during a very short time interval of the order of the 8 ns laser pulse duration. To avoid the complete evaporation of the film, an external pressure of about 0.5 to 1.0 GPa was applied, confining the sample. With the aid of the nanosecond pulsed laser, absorbed on a very thin film sample, this specially designed apparatus provides the means to produce ultrafast quenching as the formation of a plume is suppressed and heat dissipation is accelerated by the high thermal conductivity of the copper substrate and sapphire anvil. The processed samples were analyzed by microRaman spectroscopy and the results indicated the formation of polyynic carbyne structures, as revealed by the presence of a characteristic Raman peak at about  $2150\text{ cm}^{-1}$ . Another set of Raman peaks observed at 996, 1116, and  $1498\text{ cm}^{-1}$ , also appeared when the amorphous carbon film was processed with a sequence of more than three consecutive laser pulses. These peaks, whose general aspect is very similar to that of polyacetylene ( $\text{C}_n\text{H}_n$ ), could be ascribed to the cumulenic carbyne structure, stabilized by some dispersed copper atoms. © 2001 American Institute of Physics.

[DOI: 10.1063/1.1374457]

## I. INTRODUCTION

Carbon is one of the most interesting elements of nature. First of all, life is based on carbon. Secondly, the several allotropic forms of carbon have very peculiar and interesting properties.<sup>1</sup> The  $sp^3$ -allotropic form, diamond, has outstanding physical properties that make it very attractive for several scientific and technological applications. The  $sp^2$ -allotropic form, graphite, has completely different physical properties due to its layered structure. Fullerene, an alternate allotropic form of  $sp^2$  carbon, also exhibits a variety of interesting physical properties, and as such, it has been the subject of a considerable deal of basic and applied research.<sup>2</sup> The possible existence of a linear  $sp$ -allotropic form, carbyne, has been discussed in the literature since the beginning of sixties.<sup>3</sup> Carbynes consist of linear chains of carbon atoms connected by alternating triple and single bonds in the polyynic form, or connected exclusively by double bonds in the cumulenic form. Nowadays, the existence of carbynes is well supported by its assignments in Raman and infrared spectroscopy, x-ray diffraction, and transmission electron microscopy.<sup>4-9</sup> In the  $P,T$  phase diagram of carbon, the carbyne phase is considered to be stable in the low pressure and high temperature range (2600–4000 K).<sup>10</sup> Nevertheless, it

must be said that pure carbyne form has never been obtained,<sup>4</sup> and most of its physical properties, as well as crystal structure, are still unknown.

Despite the lack of fundamental knowledge about the physical properties of the  $sp$  allotropes of carbon, some possible technological applications for carbynes were proposed in the literature, including nose tips for space re-entry crafts, ultrastrong fibers, and even superconductors at an ambient temperature.<sup>8</sup> However, the main technological challenge remains in the fabrication of pure carbynes as fibers and films.

Carbynes constitute a very attractive system both from the chemical and physical points of view. There have been a great deal of efforts from both communities in achieving a better understanding of the synthesis conditions and properties of this elusive allotropic form of carbon. A search in the literature reveals several chemical and physical routes for carbyne synthesis.<sup>11</sup> The chemical procedures for carbyne preparation consist of alternative routes, most of them based on the removal of hydrogen and halogen elements from chemical structures containing carbon, leaving a carbon backbone, either polyynic or cumulenic, in nature. This transformation occurs usually at ambient pressure and temperature. Carbynes should not be stable at room temperature since they undergo spontaneous crosslinking, producing graphene structures. However, if there are terminal groups present in the reaction environment to end the carbon chains,

<sup>a)</sup>Also at: INMETRO, Av. N. Sra. Graças, 50-Xerém, RJ-25250-020-Brazil.

<sup>b)</sup>Electronic mail: naira@if.ufrgs.br

or between the chains, they would inhibit the crosslinking reactions, keeping the carbyne phase stable even at room temperature.

The physical processes usually make use of high temperature (generally higher than 2500 K), with or without high pressure (generated, for instance by shock compression), to transform graphite or amorphous carbon into carbyne. The metastable carbyne phase should be rapidly quenched to avoid crosslinking and the formation of graphite-like structures. Shock wave compression<sup>12</sup> and very high power laser<sup>13</sup> have been used to obtain carbyne. Recently, Babina *et al.*<sup>13</sup> studied the effect of the shock wave on graphite plates (sized  $25 \times 25 \times 5$  mm) and amorphous carbon samples (film  $10 \mu\text{m}$  thick), under a vacuum. In their experiments, the shock waves were produced by a pulsed Nd:YAG laser with about 70 J, pulse duration of 580 ps, and power density of  $440 \text{ GW/cm}^2$ . Transmission electron microscopy (TEM) and Auger spectroscopy analyses of the processed samples revealed the formation of relatively large closely packed crystalline carbyne. In another set of experiments, Kleiman *et al.*<sup>12</sup> studied the effect of shock compression and flash heating of graphite/metal mixtures up to 3200 K and up to 25 GPa. The high temperature and high pressure were produced by a flash heating hemispherical implosion system. The recovered samples contained diamond, graphite, and carbynes, as indicated by TEM and x-ray and electron diffraction analyses. Tanuma and Palnichenko,<sup>14</sup> trying to grow large size carbyne crystals through the direct transformation of graphite into carbyne by Joule heating of a graphite rod to temperatures higher than 2600 K, followed by a rapid cooling to room temperature, obtained, instead, what seems to be an alternate kind of allotropic form of carbon, called carbolite, consisting of *quasi*-one-dimensional carbon chains. No pressure was applied. The description of other physical processes applied to the carbyne formation can be found in a recent review paper.<sup>11</sup>

In most of the experimental physical processes found in the literature, the carbyne formation is related to the melting of a bulky carbon solid phase by shock wave or laser energy, followed by vaporization and solidification of the melted region in a cold substrate during a volumetric expansion. Despite very short heating pulses can be used, the cooling rate is limited by the thermal conductivity of the carbon samples and by the vapor plume formed by the evaporation process. In this work, we present a technique to process a very thin amorphous carbon film on a copper substrate with a high power pulsed laser in a confined sample geometry inside a high pressure cell. During the processing, with a laser pulse of 8 ns duration and up to  $2.8 \text{ MW/cm}^2$  of energy, the film is submitted to a high temperature in a very short time interval, producing ultrafast melting and quenching of the sample in nonequilibrium thermodynamic conditions. The external pressure prevents the plume expansion and evaporation, so that the quenched sample remains on the copper substrate, which accelerates the quenching rate due to the copper high thermal conductivity. The investigation about the effect of the confining geometry over the processing of the amorphous carbon film with the high power pulsed laser is one of the main goals of the present work. We estimated the maximum

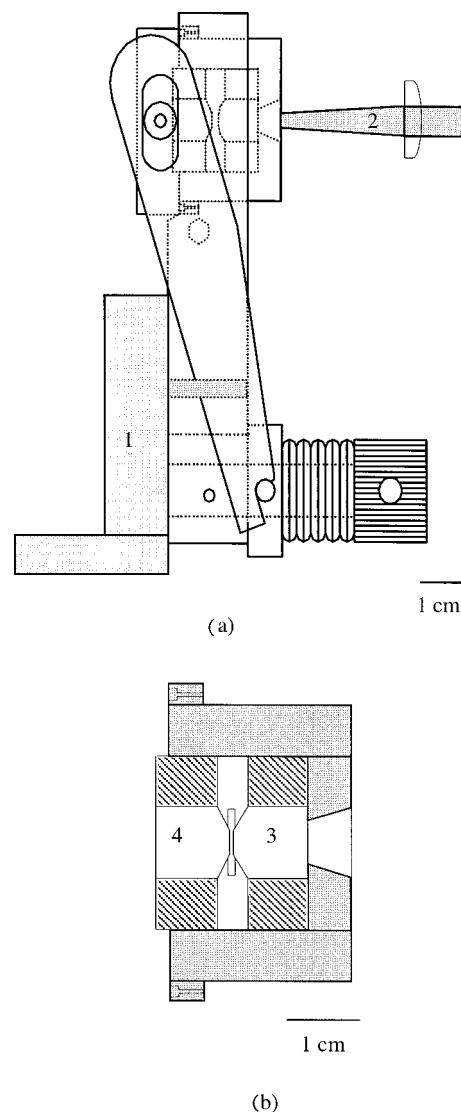


FIG. 1. High pressure cell with one anvil made of tungsten carbide and the other made of sapphire. The sapphire anvil is used as the optical window during the laser processing. (a) Schematic diagram showing the set up of the pressure cell support (1) and the laser beam firing the sampling, transpassing the sapphire anvil (2). (b) A detailed view of the anvil region, with the indented copper gasket covered by the amorphous carbon film inbetween the (3) sapphire anvil and the (4) WC anvil.

temperature reached by the thin film and the quenching rate over the copper substrate through an analytical solution for the heat diffusion equation for the two-layers system consisted by the thin film over the copper substrate. The processed films were analyzed by microRaman spectroscopy and scanning electron microscopy (SEM).

## II. EXPERIMENTAL TECHNIQUE

### A. High pressure cell

The high pressure cell was designed and constructed to submit the sample to external pressures up to 1 GPa and, simultaneously, to a high power pulsed laser beam. The cell, depicted in Fig. 1, is similar in design to the diamond anvil cell commonly used to attain high, static pressures.<sup>15</sup> However, instead of diamond anvils, it has one anvil made of

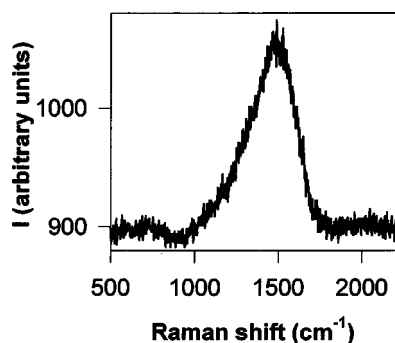


FIG. 2. Raman spectrum of the amorphous carbon film deposited on the copper gasket surface by the pulsed laser deposition technique before the laser processing.

tungsten carbide (WC) and the other made of sapphire. The diameter of the region under pressure was about 2 mm. Between the anvils it was used a copper gasket with initial dimensions of  $10 \times 10 \times 1$  mm. The carbon film was deposited over the gasket surface after a preindentation where the thickness in the central region was reduced to about 0.6 mm. The initial thickness of the carbon film, before the application of the external pressure, was about 200 nm, as estimated by side view images of the film on the substrate in SEM. After the application of the external pressure, we roughly estimate, also from SEM images, that the film thickness was reduced to about 20 nm.

The calibration of the uniaxial external pressure with respect to the turning angle of the anvil cell screw was accomplished by the  $\text{SrB}_4\text{O}_7:\text{Sm}^{2+}$  fluorescence technique.<sup>16</sup> At 1.0 GPa, a pressure gradient of the order of 0.5 GPa was observed from the center to the border of the indented region. During the laser processing, no calibrant was used to avoid the contamination of the carbon film. Also, it is expected that the internal pressure changes significantly during the high power pulsed laser.

## B. Amorphous carbon films

The amorphous carbon films were deposited on the copper gaskets by the pulsed laser deposition technique,<sup>17</sup> using a Nd:YAG pulsed laser with a repetition rate of 10 Hz. Before deposition, the pre-indented copper gasket was cleaned in an ultrasonic bath of acetone and washed with deionized water. After that, it was placed inside a vacuum chamber ( $10^{-3}$  Torr), together with a rotating graphite target. The pulsed laser beam was focused on the target surface through a spherical lens and the amorphous carbon film was deposited over the gasket. For a deposition time of 5 s, a film thickness of about 200 nm was obtained, as estimated by a side view SEM image of the copper substrate with the film. Figure 2 shows the Raman spectrum of the as-deposited film, which shows a broad band centered around on  $1450 \text{ cm}^{-1}$ , characteristic of amorphous carbon.<sup>18</sup>

## C. Processing conditions

The laser used to process the amorphous carbon film inside the high pressure cell was the same used for the film deposition. It was a Nd:YAG pulsed laser with  $1.064 \mu\text{m}$

wavelength, up to 540 mJ energy, 8 ns pulse duration full width at half maximum focused in a 1 mm region, yielding an intensity up to  $8.6 \text{ GW/cm}^2$ . Initially, the gasket with the carbon film was submitted to an external pressure of about 1 GPa inside the high pressure cell, with the film facing the sapphire anvil. The film thickness was significantly reduced to about 20 nm, crudely estimated by SEM images, but the effect of pressure was not able to modify the amorphous carbon aspect of the film, as checked with the Raman measurement of the film submitted only to the external pressure. The high power pulsed laser was focused on the film surface through an adequate alignment system and just one laser pulse hit the film. The cell was opened, the Raman spectrum of the sample was measured and, then, the same gasket was replaced inside the cell, the same pressure was applied and the sample was processed with a second laser pulse. This procedure was repeated up to 5 pulses. The same procedure was repeated for five different values for the laser pulse energy, ranging from 95 to 540 mJ ( $1.5$  to  $8.6 \text{ GW/cm}^2$ ).

Usually, after a processing with the Nd:YAG laser, the sapphire anvil was slightly damaged and impregnated with a carbon residue. Unfortunately, the coincidence of the strong sapphire fluorescence peaks with the Raman region of interest with the HeNe excitation laser used, prevented the Raman analysis of this residue. The anvil was then cleaned and polished before the next processing.

The SEM image of one of the processed samples over the copper gasket is shown in Fig. 3, where it is possible to observe nonuniformly embedded carbon clusters in the substrate.

## D. Analytical techniques

The samples, both as-prepared and after laser processed, were analyzed by microRaman spectroscopy. This technique was very suitable in this case because it did not require any sample preparation, and it permits us to get a distinctive fingerprint spectrum even for very small amounts of sample, due to the surface enhancement of the Raman signal by the copper substrate.

The microRaman spectra were excited by a HeNe laser ( $632.8 \text{ nm}$ ), 10 mW power, focused to about  $2 \mu\text{m}$  beam diameter on the sample surface. The Raman signal was collected by the microscope objective in backscattering geometry, passing through a super-Notch filter, a single-pass monochromator (0.32 m) equipped with a holographic grating (600 grooves/mm) and detected by a charge coupled device system, refrigerated by liquid nitrogen. The spectrum was recorded by a microcomputer using a specific software for data acquisition. The integration time used was 1 s to avoid any sample deterioration.

## III. RESULTS AND DISCUSSION

### A. Raman spectra and discussion

In Fig. 3, it can be seen that the morphology of the processed films was not uniform, and accordingly, the intensities of the corresponding Raman peaks were also dependent on the spot of measurement. Figure 4 shows two typical spectra of the five samples processed with different laser



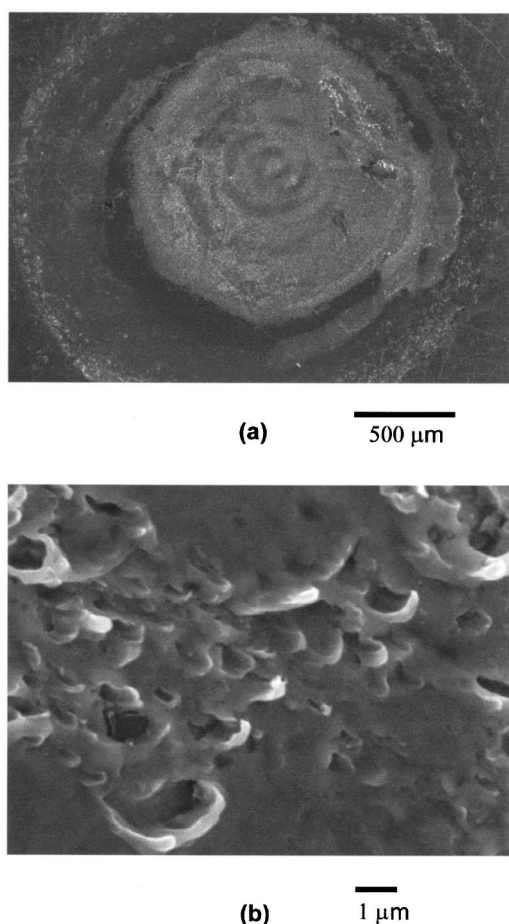


FIG. 3. SEM images of the amorphous carbon film over the copper substrate after the high power laser processing. (a) Shows the indented region of the gasket. The clearer region close to the center is where the laser hit the sample, about 1 mm diameter. Processed region with a magnification factor of 50 (a) and 10,000 (b).

pulse energy values, with one up to five laser pulses. The Raman spectra of all processed samples, in several spots of the same sample, were very similar to each other, without any systematic changes related to the laser pulse energy used. The amorphous carbon spectrum (Fig. 2) of the initial film was not recovered in any spot inside the processed region. A disordered graphite spectrum was usually found in most spots, as indicated by the broad bands at  $\sim 1330$  and  $1580\text{ cm}^{-1}$ . Together with the graphite spectrum there is a band at about  $2150\text{ cm}^{-1}$ , associated to a triple bond of carbon atoms ( $\text{C}\equiv\text{C}$ ). This band is usually attributed to carbynes,<sup>5</sup> being, in fact, related to the polyynic kind of carbyne. The magnitude of this carbyne band changed for different spots but it was stable under the action of the HeNe laser. The band at about  $400\text{--}600\text{ cm}^{-1}$  could probably be related to disorder induced Raman scattering of nanocrystalline carbon, as suggested in Ref. 19, although it was not possible to identify it precisely with the available information.

The processing of the film with only one laser pulse was enough to destroy the amorphous film and to produce a sample with a graphite-like Raman spectrum. Even in this situation, a small peak was already observed close to  $2150$

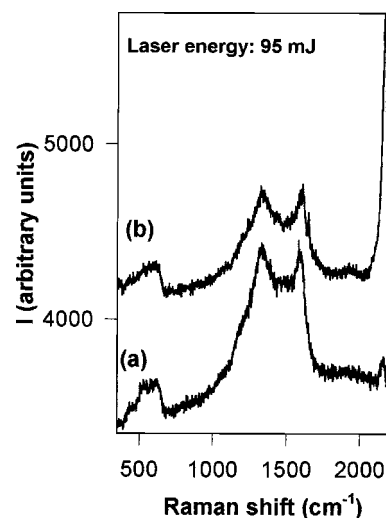


FIG. 4. Raman spectrum of the processed region of the film with a laser pulse of 95 mJ. It is shown the spectra after one single pulse (a) and after four nonconsecutive pulses (b).

$\text{cm}^{-1}$ , indicating the formation of triple bond carbon vibrations. Subsequent laser pulses, one at a time, increased the intensity of this Raman peak. This effect is probably related to the gradual transformation of the graphite-like structure, formed during the action of the first laser pulse, to a carbyne-rich moiety perhaps due to the incorporation of Cu atoms, which is known to stabilize the carbyne structure.<sup>4</sup>

Akagi *et al.*<sup>20</sup> proposed the following relationship to estimate the carbyne chain length from the triple bond stretching frequency ( $\nu_{\text{C}\equiv\text{C}}$ ):

$$n = \frac{698}{\nu_{\text{C}\equiv\text{C}} - 2104} - 1, \quad (1)$$

where  $n$  is the number of carbon atoms in the chain, and the frequency is given in  $\text{cm}^{-1}$ . Using the  $\nu_{\text{C}\equiv\text{C}}$  frequency values found for all the samples studied, ranging from  $2145$  to  $2165\text{ cm}^{-1}$ , we found that the linear chains should contain from 11 to 16 carbon atoms.

It was observed that when the amorphous carbon film deposited on the copper gasket was processed outside the cell, in a nonconfined geometry, only graphite-like structures were formed, without any indication of polyynic carbyne. In other words, no carbyne formation was observed without the applied external pressure to confine the high temperature plasma.

Figure 5 shows the Raman spectra for another set of films processed with five consecutive laser pulses at a repetition rate of 0.5 Hz, each sample processed with a different laser pulse energy. When the laser energy was not very high and the maximum temperature was up to  $10\,000\text{ K}$  [see Fig. 6(a)], it was observed, besides disordered graphite and the  $\sim 2150\text{ cm}^{-1}$  band, two sharp and strong peaks at about  $1116$  and  $1498\text{ cm}^{-1}$ , followed by a smaller peak at  $\sim 996\text{ cm}^{-1}$ . These peaks always appeared simultaneously and their intensities were very unstable under the action of the HeNe laser. They were not detected for the case of processing with only one pulse, but they continue to appear for processing with more than five pulses consecutively.

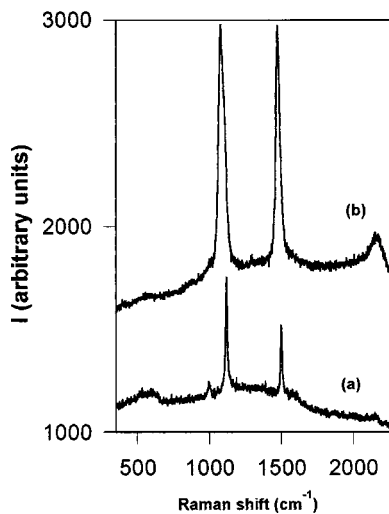


FIG. 5. Raman spectrum of the processed region of the film with a laser pulse of 230 mJ after five consecutive pulses (a), (b) Polyacetylene Raman spectrum, for comparison.

## B. Temperature calculation

The direct measurement of the sample temperature during the laser pulse processing is complicated due to the very short pulse time interval and the geometrical constraints: the sample was located inside the pressure cell, visible only throughout the small sapphire window oriented to the incident laser radiation. Consequently, in order to estimate the magnitude of the sample temperature during laser processing, we considered an available theoretical model providing the solution for the heat diffusion equation with boundary conditions compatible to our experimental setup, taking explicitly into account the effect of the film substrate. More specifically, we selected the solution given by Matricon<sup>21</sup> for the heat diffusion across a two-layer system consisting of a thin film in ideal thermal contact with a semi-infinite substrate. In this model, the thin film surface is supposed to be uniformly heated by the heat source given by  $q(t) = q_0$  for  $t \leq \tau$ , and  $q(t) = 0$  for  $t > \tau$ , where  $\tau$  is the pulse time duration ( $\tau = 8.5$  ns in the present case), and  $q_0$  is the power density delivered by the laser pulse. The thermal parameters required to calculate the temperature are shown in Table I, and we assumed they are independent of temperature, as a first approximation. In the case of the amorphous carbon film, the thermal properties are strongly dependent on the film preparation process and we could not find consistent values for them in the literature, so we considered the graphite properties in a first approximation. Figure 6(a) shows the

TABLE I. Physical parameters used in the temperature calculation from an analytical solution of the heat diffusion equation for a graphite thin film over a copper substrate when the laser pulse energy was deposited on the film surface.

Parameter	Graphite	Copper
density (kg m <sup>-3</sup> )	2260	8933
thermal conductivity (W m <sup>-1</sup> K <sup>-1</sup> )	6.3	416
heat capacity (J kg <sup>-1</sup> K <sup>-1</sup> )	700	386
thickness (nm)	20	semi-infinite

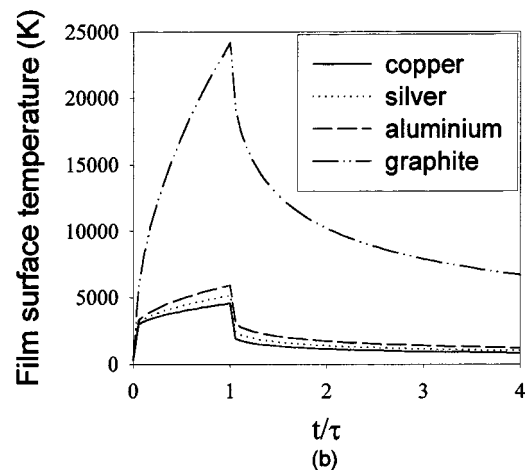
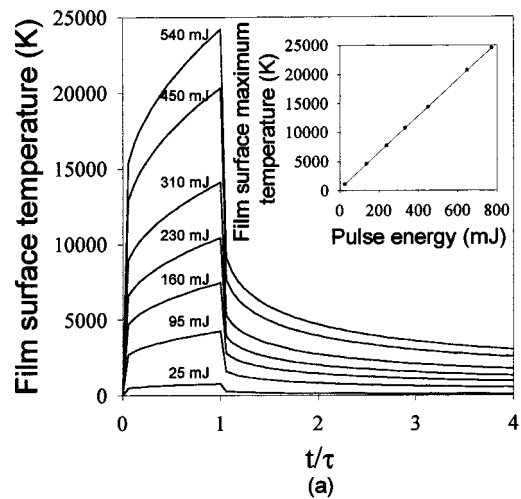


FIG. 6. (a) Maximum temperature as a function of time,  $t/\tau$ , where  $\tau$  is the temporal laser pulse width, considering the available laser pulse energies. These results were obtained from an analytical solution of the heat diffusion equation for a graphite thin film over a copper substrate when the laser pulse energy was deposited on the film surface. (b) Maximum temperature as a function of  $t/\tau$  considering different substrates for the graphite thin film.

estimated maximum temperature reached by the film for the different values of the laser pulse energy used in the experiments. The temperature rise rate and maximum temperature depend on the thermal properties of the thin film and, also, on the thermal properties of the copper substrate. In the present case, the copper substrate dissipates the heat very efficiently due to its high thermal conductivity. The maximum temperature is not as high as it could be if the film was in a substrate with lower thermal conductivity, such as aluminium or graphite. Figure 6(b) shows the maximum temperature calculated for the film surface on selected substrate materials for a laser pulse energy of 95 mJ. It is interesting to point out that the time required to cool the temperature down to half the maximum value in the case of the copper substrate is about 20 times smaller than in the case of the graphite substrate. Therefore, the processing of the thin amorphous carbon film over a copper substrate in a confined geometry provided a very high temperature and, also, a very high cooling rate, without evaporation and condensation.

We would like to point out that this model did not take into account the sapphire anvil contribution to the tempera-

ture and quenching rate calculations, therefore the results should be considered as estimated values. In fact, despite the sapphire anvil will contribute reducing the maximum temperature and increasing the heat dissipation rate, the thermal diffusivity of the copper substrate is about 25 times higher than that of sapphire.<sup>22,23</sup> This reduces considerably the impact of adding the sapphire anvil contribution to our calculations.

### C. Substrate effect

In order to study the substrate effect on the sample processing, we processed the amorphous carbon film over alternative substrates such as silver and copper coated with thick titanium and gold films. The band at  $\sim 2150\text{ cm}^{-1}$  always persisted but the sharp Raman peaks did not appear for any one of these cases, suggesting a close dependence on the copper substrate itself. The experiment with aluminum gasket was catastrophic since the aluminum welded in the sapphire anvil, with the amorphous film inbetween them, due to the high temperature reached [see Fig. 6(b)]. The silver gasket did not weld on the sapphire but the sharp Raman peaks were not observed.

On the other hand, when the thin amorphous carbon film was deposited on the copper substrate using an acetylene flame or a candle soot, instead of by the pulsed laser deposition technique, the same sharp peaks of Fig. 5 appeared for processing with consecutive laser pulses.

### D. Characterization of the processed sample

In the literature, it was found that the Raman spectrum of polyvinyl chloride (PVC) treated with an UV laser to remove the hydrogen and chlorine atoms, leaving a carbon structure at the PVC surface,<sup>24</sup> is very similar to the one shown in Fig. 5, with the same Raman peaks. The authors attributed their spectrum to a polyacetylene like structure, due to the presence of remaining hydrogen atoms. The spectrum of polyacetylene is shown in Fig. 5 for comparison.

In order to investigate the reason for the very close coincidence of the Raman spectra of our processed sample and of the UV treated PVC, attributed to polyacetylene by the authors, we performed some tests to confirm or discard the hydrogen contamination of our sample. The first test consisted in the evaluation of the hydrogen content of the as-deposited amorphous carbon film: the film was deposited on a silicon substrate, using the same deposition conditions, and we measured the CH absorption band intensity by infrared spectroscopy. The intensity of this band was negligible, indicating that there was practically no hydrogen content in the as-deposited amorphous carbon film. During the laser processing in a confined geometry, there was no obvious interaction of the film with hydrogen, except by the interaction with atoms from the atmosphere.

The second test consisted of an increase in the hydrogen content in the processed region by adding some water close to the copper gasket. In this case, the sharp Raman peaks were not observed. Finally, we considered the effect of isotopic substitution on the Raman spectrum of polyacetylene which is well known, and it was used as another test to verify

the presence of  $C_nH_n$  in our samples. It was expected that, if the processed carbon films contained a polyacetylene-like structure, with hydrogen atoms, the Raman peaks would shift by substituting deuterium for hydrogen. Several attempts were made to promote this isotopic substitution, including the deposition, over the copper substrate, of an amorphous carbon film generated by burning of deuterated acetylene and also laser processing of a carbon film in an environment containing deuterium oxide. In any case, none of these attempts resulted in changes in the Raman spectra of the laser processed carbon films that could be ascribed to the effect of isotopic substitution. These results, together with the absence of CH bands in the infrared spectrum of the as-prepared amorphous carbon films, ruled out the possibility of polyacetylene synthesis in our experiments. We, therefore, propose the formation of a new phase, probably an unstable cumulenic carbyne, with sharp Raman peaks at 996, 1116, and  $1498\text{ cm}^{-1}$ , in addition to the formation of the more stable polyyinic carbyne, evidenced by the carbon triple bond Raman peak at about  $2150\text{ cm}^{-1}$ . Previous works<sup>4</sup> have suggested that some dispersed copper atoms would stabilize the carbyne phase, preventing the crosslinking and graphene-like reconstruction of the carbon backbone. On the other hand, the polyyinic carbyne moiety seems to be independent of the copper substrate, since its Raman spectrum was found also when the amorphous carbon film was deposited on silver substrates.

We searched in the literature for the vibrational spectra of known compounds containing carbon and copper or hydrogen atoms, considering only linear structures of the following kinds:  $C_nH_m$ ,  $Cu_nC_m$ ,  $C_n$ , and  $Cu_n$ , where  $n$  and  $m$  are integer numbers. We did not find any compound whose vibrational spectrum could fit the Raman peaks shown in Fig. 5. From the searched vibrational spectra, the Raman spectrum of allene ( $C_3H_4$ ) is the closest to the one measured for the product obtained in our experiments.<sup>25</sup> It is difficult to find information about the vibrational spectra of copper-carbide small clusters since there is a very small amount of work about this subject.<sup>26</sup>

The processed sample probably does not consist of inorganic compounds such as aluminum carbides or oxycarbides, which are usually stable at high temperatures. In fact, when the copper gasket containing the processed carbon film were heated up to  $100^\circ\text{C}$  in a vacuum during 1 h, the sharp Raman peaks were completely eliminated. Furthermore, the intensity of these peaks decreased by the action of the HeNe/laser during the Raman measurements. This thermal instability is generally observed for organic compounds.

Some hypothesis regarding the nature of the product obtained in these laser irradiation experiments were checked by means of *ab initio* calculations using the Cambridge analytical derivative package—CADPAC. The computations were carried out at the Hartree–Fock level, using standard Pople's 3–21 G basis set for both carbon and copper atoms. In these calculations, we obtained estimates for the frequencies and relative intensities of Raman-active vibrational modes for some small copper-ended linear carbon chains such as:  $Cu_4C_2$ ,  $Cu_4C_3$ ,  $Cu_4C_4$ , and  $Cu_4C_7$ . In the specific case of a three-carbon chain ended by two copper atoms at each side,

the Raman shift of the more intense modes were located at 1034, 1444, and 1970  $\text{cm}^{-1}$ . This result, closely resembling our experimental observation, suggests that small molecules containing carbon and copper, similar to copper acetylide, could be formed in the process of laser irradiation and rapid quenching. These small molecules, having a carbyne backbone, would be stabilized by the copper atoms at their ends, thus preventing the crosslinking between neighbor chains. The calculated C—C distance was inbetween the C=C and C≡C typical values, indicating a resonant hybridization between these two states.

Despite the *P,T* conditions to the carbyne formation should be very close to the fullerene conditions,<sup>4</sup> it was not observed any indication of fullerene formation in the Raman spectra. The ultrafast quenching during the high power laser processing probably induces the formation of linear structures only. Moreover, if there are free radicals in the reaction environment to prevent the crosslinking of the linear chains, the fullerene formation would be suppressed in favor of the carbyne chains.<sup>14</sup> The formation of nanocrystalline diamond was not observed in the Raman spectra but it was not discarded.

#### IV. CONCLUSIONS

We presented a technique suitable to produce an ultrafast temperature quenching of thin films under pressure using a high power pulsed laser. The effect of this quenching on amorphous carbon films was investigated through Raman spectroscopy. During the laser pulse, the temperature was very high and the plume expansion was suppressed by the external pressure. It was found that the substrate plays an important role in the maximum temperature reached, in the cooling process and, also, in the phase transformation of the amorphous carbon film during the pulsed laser processing.

The spectroscopic analysis of the processed films revealed the formation of polyynic carbyne, and, additionally, a second phase was observed by Raman spectroscopy, very similar to polyacetylene. Several approaches were investigated in order to elucidate the origin of this second phase, constrained by the nanometric sample size. There was no success in trying to experimentally confirm the polyacetylenic structure. It was observed that this second phase depends on the copper substrate itself, and it probably contains

some copper atoms in its structure. Some theoretical calculations suggest the formation of small carbon-copper clusters, with a linear carbon arrangement, similar to cumulenenic carbyne.

#### ACKNOWLEDGMENTS

The authors are grateful for the financial support of PADCT/CNPq, FAPERGS, FINEP, CNPq, and CAPES from Brazil.

- <sup>1</sup>*Handbook of Carbon, Graphite, Diamond and Fullerenes, Properties, Processing and Applications*, edited by H. O. Pierson (Noyes Publications, Park Ridge, NJ, 1993).
- <sup>2</sup>International Winterschool on Electronic Properties of Novel Materials, *Progress in Fullerene Research*, edited by H. Kuzmany, J. Fink, M. Mehring, and S. Roth (World Scientific, Singapore, 1994).
- <sup>3</sup>P. P. K. Smith and P. R. Buseck, *Science* **216**, 984 (1982); L. Kavan and J. Kastner, *Carbon* **32**, 1533 (1994).
- <sup>4</sup>F. Cataldo and D. Capitani, *Mater. Chem. Phys.* **59**, 225 (1999).
- <sup>5</sup>L. Kavan, J. Hlavaty, J. Kastner, and H. Kuzmany, *Carbon* **33**, 1321 (1995).
- <sup>6</sup>F. Cataldo, *Eur. J. Solid State Inorg. Chem.* **35**, 293 (1998).
- <sup>7</sup>F. Cataldo, *Eur. J. Solid State Inorg. Chem.* **34**, 53 (1997).
- <sup>8</sup>F. Cataldo, *Polym. Int.* **44**, 191 (1997).
- <sup>9</sup>Y. Ando, *Carbon* **33**, 171 (1995).
- <sup>10</sup>A. G. Whittaker, *Science* **200**, 763 (1978).
- <sup>11</sup>Y. P. Kudryavtsev, R. B. Heimann, and S. E. Evsyukov, *J. Mater. Sci.* **31**, 5557 (1996).
- <sup>12</sup>J. Kleinman, R. B. Heimann, D. Hawken, and N. M. Salansky, *J. Appl. Phys.* **56**, 1440 (1984).
- <sup>13</sup>V. M. Babina, M. Boustie, M. B. Guseva, A. Z. Zhuk, A. Migault, and V. V. Milyavskii, *High Temp.* **37**, 543 (1999).
- <sup>14</sup>S. Tanuma and A. Palnichenko, *J. Mater. Res.* **10**, 1120 (1995).
- <sup>15</sup>*High Pressure Experimental Methods*, edited by M. I. Eremets (Oxford University Press, New York, 1996).
- <sup>16</sup>A. Lacam and C. Chateau, *J. Appl. Phys.* **66**, 366 (1989).
- <sup>17</sup>P. R. Willmott and J. R. Huber, *Rev. Mod. Phys.* **72**, 315 (2000).
- <sup>18</sup>M. Chhowalla, A. C. Ferrari, J. Roberston, and G. A. J. Amaratunga, *Appl. Phys. Lett.* **76**, 1419 (2000).
- <sup>19</sup>F. Li and J. S. Lannin, *Appl. Phys. Lett.* **61**, 2116 (1992).
- <sup>20</sup>K. Akagi, M. Nishiguchi, and H. Shirakawa, *Synth. Met.* **17**, 557 (1987).
- <sup>21</sup>M. Matricon, *J. Phys. Radium* **12**, 15 (1951).
- <sup>22</sup>P. H. Sidles and G. C. Danielson, *J. Appl. Phys.* **25**, 58 (1954).
- <sup>23</sup>*Handbook of Materials Science*, Vol. III, Metals, Composites and Refractory Materials, edited by Charles T. Lynch (CRC, Cleveland, Ohio, 1975), p. 360.
- <sup>24</sup>M. Shimoyama, H. Niino, and A. Yabe, *Makromol. Chem.* **193**, 569 (1992).
- <sup>25</sup>C. Liang, Y. Xie, H. F. Schaefer, III, K. S. Kim, and H. S. Kim, *J. Am. Chem. Soc.* **113**, 2452 (1991).
- <sup>26</sup>Y. Yamada and A. W. Castleman, Jr., *Chem. Phys. Lett.* **204**, 133 (1992).